Preparation of Novel Complex Nano-Structured Gold Catalyst Au@TiO₂/MCM-22, Characterization and Remarkably Catalytic Performance for Cyclohexane Oxidation

Jiaqi Si, Lin Li, Yanji Zhang, Ji-Cheng Zhou*, Wenbing Ouyang

Key Laboratory of Green Catalysis and Reaction Engineering, Department of Education, College of Chemical Engineering, Xiangtan University, Xiangtan, China
Email: *zhoujicheng@sohu.com

Abstract

A novel complex nano-structured Au@TiO₂ gold catalyst has been prepared. Au precursor could be transformed into Au@TiO₂/MCM-22 with the complex nano-structured using two different methods. Samples were characterized by XRD, FT-IR, UV-vis, TEM, ICP-AES and N_2 adsorption-desorption. It is found that gold was anchored on the TiO₂/MCM-22 as small size and uniform particles with the average diameters in the range of 5 - 9 nm. Catalytic results show that such nano-gold catalysts display excellent catalytic performance for cyclohexane oxidation. Au@TiO₂/MCM-22 catalyst with the gold content of 0.5 wt% exhibits extremely exceptionally catalytic activity (12.81%) and high turnover frequency (52,121 h^{-1}), which may be ascribed to the synergistic effects of Au and TiO₂ in the complex nano-structured catalyst Au@TiO₂/MCM-22. Because of the strong metal support interaction, aggregation of active sites (Au nanoparticles) during the oxidation reaction is effectively prohibited and the catalytic activity is essentially retained.

Keywords

Complex Nano-Structured Catalyst, Photocatalytic Reduction Method, Au@TiO₂/MCM-22, Gold Nanoparticles, Cyclohexane Oxidation

1. Introduction

The popular of nanoscience has exploded within the last two decades, mainly because new nano-synthesis processes have led to a wealth of novel nanostruc-

tures with adjustable size and shape parameters, leaving researchers with extraordinary control over their chemical properties. Metal-oxide hybrid nanoparticles are quite interesting and popular among novel nanostructures [1] [2]. The materials systems are expanded from single-component nanoparticles to hybrid multicomponent heteronanostructures which integrate discrete domains of different compositions within one hybrid nanostructured entity [3] [4] [5]. Metal-oxide hybrid nanoparticles represent an important class of multicomponent nano-systems that may exhibit not only a combination of properties from the individual components but also further enhanced property and even new synergistic properties which arise essentially from the nanoscale interactions between the disparate metal and oxide components [6]. Two fundamental explanations of interaction between metal-oxide are proposed, so-called interfacial charge redistribution-electronic interaction [7] [8] and interfacial atom transport-chemical interaction [9] [10]. Furthermore, such nanoparticles defined by a diameter of 1 - 10 nm, are creating a new category of materials, which is different either from conventional bulk materials or from atoms, the smallest units of matter [11] [12]. Thus, oxide supporting with ultrafine metal nanoparticles have tremendous prospects.

Tauster *et al.* [13] proposed the strong metal-support interaction (SMSI) firstly in 1978 to explain the suppression of H_2 and CO chemisorption capacity of metal cluster on TiO_2 chemically reduced at high temperatures. Since then, a large number of researches in catalysis have been reported, and they have extensively demonstrated that the SMSI in supported group VIII metal plays a prominent role in catalytic performances [14] [15]. The SMSI states are mainly influenced by two factors: geometric and electronic. The geometric factor is due to encapsulation, which results from a physical covering of metal particles by a thin layer of reduced oxide support (e.g. TiO_2, V_2O_5, SiO_2 and Al_2O_3) [16]. The electronic factor is determined by a perturbation (for example, a charge transfer between the metal and the oxide) of the electronic of the metal catalyst [17]. It is reported that the metals with high surface energy such as Pt and Pd are more likely to be encapsulated than those with low surface energy (e.g. Au and Cu) [18].

The selective oxidation of cyclohexane to cyclohexanone and cyclohexanol is one of the most compelling researches in the field of catalytic chemical research, for the oxidation products (cyclohexanone and cyclohexanol) are very important chemical raw materials and intermediates, mainly for the production of adipic acid and caprolactam, which is the monomer of nylon-6 and nylon-66, respectively [19] [20]. Metal-oxide hybrid nanoparticles have been applied to cyclohexane oxidation in the literature. Zhu *et al.* [21] [22] [23] prepared Au/Al_2O_3, $Au/Al_2O_3/SiO_2$ and $Au/TiO_2/SiO_2$ catalysts by deposition precipitation method, and the good results of cyclohexane oxidation suggested that gold supported on the oxides might be superior catalysts. However, turnover frequency (TOF) of these catalysts is relatively low and reaction time is long.

Herein, we report a novel complex nano-structured $Au@TiO_2$ catalyst pre-

pared by photocatalytic reduction method and deposition precipitation method. In particular, Au nanoparticles with a diameter around 7 nm are well-decorated on the TiO_2/MCM-22 surface. The as-synthesized Au@TiO_2/MCM-22 nano-composites are used for cyclohexane oxidation. For the synergistic effects of Au and TiO_2 in the nano-Au@TiO_2 hybrid structure, Au@TiO_2/MCM-22 has enhanced catalytic activity remarkably for oxidation of cyclohexane. The recyclability tests display that the as-synthesized catalyst has strongly chemical and mechanical stability. Supported noble metal nanoparticles catalysts (Pd, Pt, Ru, etc.) with nano-Me@TiO_2 complex structure could be also prepared and applied into different reaction system.

2. Experimental

2.1. Catalyst Preparation

2.1.1. Preparation of TiO_2/MCM-22 by Sol-Gel

The MCM-22, referring to Wang *et al.* [24] using hexamethyleneimine (HMI) as template, was synthesized. A certain amount of MCM-22 (1.00 g) and 5 mL of tetrabutylammonium titanate (TBOT) were dissolved together in ethanol (15 mL), and the solution was stirred at 300 rpm at 293 K for 12 h. Then a small amount of HNO_3 was added under stirring. After aging for 24 h at ambient temperature and drying for 24 h at 363 K, the resulting mixture was calcined for 3 h at 823 K thermostatically. According to principles of the spontaneous mono-layer distribution, metal oxide would disperse on the support with a state of the spontaneous monolayer distribution, when the content of metal oxide is less than a certain threshold. Thus, the TiO_2 loaded on the MCM-22 could form a monolayer or multilayers, which could be achieved by adjusting the loading of TiO_2.

2.1.2. Preparation of Au@TiO_2/MCM-22 by Photocatalytic Reduction Method

Typically, 0.5% Au@TiO_2/MCM-22 (PR) catalyst were prepared as follow: the prepared TiO_2/MCM-22 samples (1.00 g) were dispersed in 100 mL distilled water and treated by ultrasonic agitation for 10 min. The slurry was transferred into the reactor, and distilled water was added to dilute the mixture to 90 mL and stirred for 1 h. Subsequently, $HAuCl_4 \cdot 4H_2O$ (0.1050 g) were added. Two drops of HNO_3 solution were added to adjust the pH to 3; the suspension was irradiated with a 15 W UV lamp for 4 h. Finally, the samples were separated by filtration, washed several times by distilled water, dried for 4 h at 355 K. The obtained material was denoted by Au@TiO_2/MCM-22 (PR).

2.1.3. Preparation of Au@TiO_2/MCM-22 by Deposition Precipitation Method

Typically, 0.5% Au@TiO_2/MCM-22 (DP) catalyst were prepared as follow: $HAuCl_4 \cdot 4H_2O$ (0.1050 g) were added into the mixer of TiO_2/MCM-22 (1.00 g) and distilled water (90 mL), which was mixed uniformly by ultrasonic. After adjusting pH to 9.0 with NaOH solution, the solution was stirred for 4 h in dark.

The suspension was filtrated, washed by distilled water, dried at 255 K, and calcined at 523 K for 6 h. The obtained material was denoted by Au@TiO$_2$/MCM-22 (DP).

2.2. Catalyst Characterization

The nitrogen cryogenic adsorption isotherms were obtained on an AUTOSORB-1-MP-type physical adsorption instrument. Specific surface area measured by BET method, pore size distribution and pore volume calculated by the BJH method. The chemical compositions of the samples were determined by ICP-AES (IRIS Intrepid II XSP). Fourier transform infrared (FT-IR) spectroscopy measurement was recorded on Nicolet 380 equipment, using KBr pellet method. X-ray Diffraction (XRD) patterns were collected on a D/max-3c diffract meter operated at 100 mA and 40 kV. The step size was 0.02 degree and the step time was one min. Transmission electron microscopy (TEM) images were obtained on a JEM-2010 at 160 kv. UV-Vis spectroscopy measurement was recorded on Japan UV-2550 equipment.

2.3. Catalytic Reaction Experiments

In a typical oxidation reaction, 100 mL cyclohexane, 0.08 g catalyst and 0.4 g tert-butyl hydrogen peroxide (TBHP) as initiator were added in a 300 mL autoclave reactor. The reactor was heated to 423 K and the O$_2$ pressure was adjusted to 1.0 MPa. After 1.0 h of reaction, the liquid was extracted from the autoclave and the catalysts were separated. The product of cyclohexanol and cyclohexane were analyzed by gas chromatograph (Agilent 6890N) with internal standard method using chlorobenzene as the standard substance. The concentration of cyclohexyl hydroperoxide (CHHP) was analyzed by iodometric, and the acids and esters were determined by acid-base titration.

3. Results and Discussion

3.1. Characterization

3.1.1. N$_2$ Adsorption-Desorption Isotherms
Table 1 shows the N$_2$ adsorption-desorption isotherms of the as-prepared samples. A dramatic decrease of the specific surface area can be discerned after doping of TiO$_2$, while there are only mild decreases in pore volume. This can be the reason of that TiO$_2$ is layered dispersion in the bore wall of the MCM-22 hole rather than a cluster state. Moreover, after loading gold, the pore size of TiO$_2$/MCM-22 is decreased slightly. This is mainly because a part of pores of TiO$_2$/MCM-22 may be blocked by the depositing of gold onto the substrate [25] [26].

3.1.2. ICP-AES Analysis
The Au loading efficiency of prepared samples is revealed by ICP-AES in Table 2. It is evident that modifying MCM-22 with TiO$_2$ is useful to improve the loading of Au indeed (Table 2, Entry 1 and 2), and this is consistent with Xu *et al.* [22]. Entry 2 and 5 in Table 2 show that photocatalytic reduction method can

Table 1. Textural properties obtained from N_2 physisorption.

Sample	$S_{BET}/m^2 \cdot g^{-1}$	$V_{BJH}/cm^3 \cdot g^{-1}$	D^a_{BJH}/nm
MCM-22	352	0.24	1.25
TiO$_2$/MCM-22	275	0.22	1.25
Au@TiO$_2$/MCM-22 (PR)	273	0.22	1.20

[a]Calculated from the adsorption branch of the nitrogen adsorption and desorption isotherms. Au: 0.5 wt%.

Table 2. Loading efficiency of Au nanoparticles under different conditions.

Entry	Catalysts	Illumination time (h)	Nominal Au (wt%)	Actual Au (wt%)	m (Catalyst)/g	Loading efficiency[b]
1	Au/MCM-22	4	0.5	0.21	0.843	35.4%
2	Au@TiO$_2$/MCM-22 (DP)	4	0.5	0.32	0.864	55.3%
3	Au@TiO$_2$/MCM-22 (PR)	4	0.1	0.14	0.708	99.1%
4	Au@TiO$_2$/MCM-22 (PR)	4	0.2	0.24	0.845	101.4%
5	Au@TiO$_2$/MCM-22 (PR)	4	0.5	0.46	0.909	83.6%
6	Au@TiO$_2$/MCM-22 (PR)	2	1.0	0.62	0.820	50.8%
7	Au@TiO$_2$/MCM-22 (PR)	4	1.0	0.82	0.861	70.8%
8	Au@TiO$_2$/MCM-22 (PR)	6	1.0	1.13	0.841	95.0%
9	Au@TiO$_2$/MCM-22 (PR)[a]	4	0.5	0.46	0.910	83.7%

[a]Au@TiO$_2$/MCM-22 (PR) (repeated use four times). [b]Loading efficiency = Actual Au * m (catalyst)/Nominal Au * 1.00 (1.00: theoretical mass of the catalyst).

enhance the loading efficiency of Au significantly, compared with deposition precipitation method. The gold loading on Au@TiO$_2$/MCM-22 (PR) doesn't alter basically, even after being utilized four times (**Table 2**, Entry 5 and 9). Nominal Au raises the Au loading but obviously reduces the loading efficiency (**Table 2**, Entry 3, 4, 5 and 7). This may be the result of deficient illumination time. Perhaps because of the loss of the support during preparation, the loading efficiency exceeds 100% (**Table 2**, Entry 3 and 4). With the growth of illumination time, the loading efficiency is also improved (**Table 2**, Entry 6, 7 and 8), which indicates that the ample illumination time could achieve gold load entirely.

3.1.3. XRD Analysis

The X-ray diffraction (XRD) patterns of TiO$_2$/MCM-22, Au@TiO$_2$/MCM-22 (DP) and Au@TiO$_2$/MCM-22 (PR) are shown in **Figure 1**. It is obvious that all the samples have some similar peaks. The peaks at $2\theta = 25.3°$, 38.2°, 48.1°, 53.5°, 55.1°, 62.7°, 68.8°, 70.3° and 75.8° can be indexed to crystallite planes of (101), (004), (200), (105), (211), (204), (116), (220) and (215), respectively, which are ascribed to the anatase-TiO$_2$ (JCPDS card No. 21-1272) [27]. The diffraction peaks at 2θ of 38.3°, 44.4°, 64.6° and 77.6° (**Figure 1(c)** and **Figure 1(d)**) are corresponding to (111), (200), (220), (311) Au plane, respectively, according to JCPDS card No. 76-1082 [28]. Notably, no typical diffraction peaks belonging to the Au are observed in the Au@TiO$_2$/MCM-22 (DP) nanocomposites. The reason can be
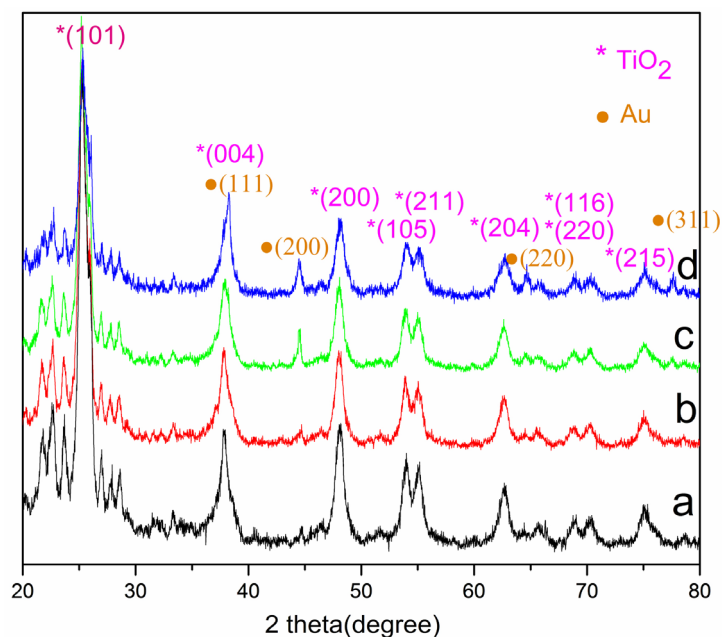
Figure 1. X-ray diffraction pattern of samples. (a) TiO_2/MCM-22; (b) Au@TiO_2/MCM-22 (DP); (c) Au@TiO_2/MCM-22 (PR); (d) Au@TiO_2/MCM-22 (PR) (repeated use four times). Au: 0.5 wt%.

ascribed to the poor weight loading of metal nanoparticles on the TiO_2/MCM-22 by deposition precipitation. In particular, after being used for four times, the Au@TiO_2/MCM-22 (PR) sample still exhibits the typical signals of Au, which is in accordance with the ICP-AES result.

3.1.4. FT-IR Spectra

Figure 2 shows the FT-IR spectra of the prepared catalysts. It can be seen that there are strong absorption bands at 3440 and 1630 cm^{-1}, which can be assigned to stretching vibration of −OH of adsorbed water and the vibration of Si-O-H bond [29], respectively. The stretching vibration of Si-O-Si is the cause of bands position around 460 and 1080 cm^{-1} [30]. Two additional absorption peaks at 965 and 557 cm^{-1} are attributed to the vibration of the newly-formed Si-O-Ti bond in the spectrum of TiO_2/MCM-22 and Au@TiO_2/MCM-22 (PR) [31] [32] which indicate that the TiO_2 has doped on the framework of MCM-22.

3.1.5. TEM Images

TEM images and Au nanoparticles size distribution histograms of prepared gold catalysts are shown in **Figure 3**. The gold nanoparticles are evident as small dark spots, while the TiO_2/MCM-22 substrate is brighter and larger. Apparently, gold assembles together on MCM-22, and the diameter range of gold particles is rather broad (**Figure 3(a)**). The Au@TiO_2/MCM-22 (DP) sample shows that modifying MCM-22 with TiO_2 could decrease the loaded gold nanoparticles size (6 - 10 nm) remarkably (**Figure 3(b)**). Au nanoparticles are successfully immobilized on the TiO_2/MCM-22 with a diameter around 5 - 9 nm (**Figure 3(c)**). After being utilized four times, the Au@TiO_2-MCM-22 (PR) still maintains the original
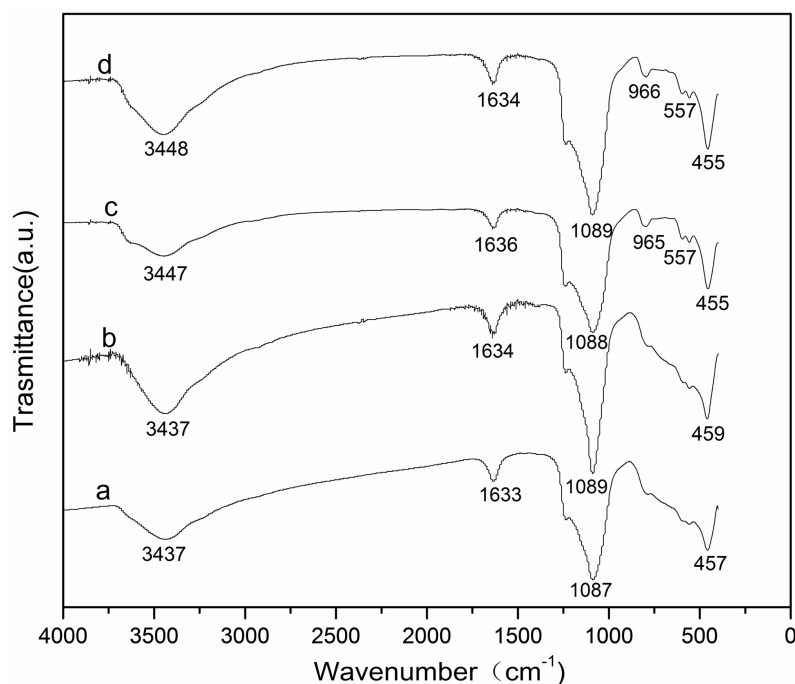
Figure 2. FT-IR spectra of samples. (a) MCM-22; (b) Au/MCM-22; (c) TiO$_2$/MCM-22; (d) Au@TiO$_2$/MCM-22 (PR). Au: 0.5 wt%.

morphology, which suggests that the gold nanoparticles load on the support stably (**Figure 3(d)**). Therefore, photocatalytic direct reduction is an effective method to obtain small size, well dispersion and stable structure nanoparticles.

3.1.6. UV-Vis Spectra

UV-visible spectroscopy is an effective method for characterizing the composition and structure of catalysts. **Figure 4** shows the UV-vis spectra of MCM/22, Au/MCM-22, Au@TiO$_2$/MCM-22 (DP) and Au@TiO$_2$/MCM-22 (PR). Generally, a broad absorption band in the visible region around 520 nm is typical for the surface plasma resonance (SPR) of nano-sized gold [33]. Samples MCM-22 and TiO$_2$/MCM-22 exhibit featureless spectrum because of the absence of gold. It was reported that with the increase of Au particle size, the SPR peak shifts to longer wavelength or intensifies at longer wavelength [34] [35], that is, the original peak became broader due to the coupling of the individual surface Plasmon of nanoparticles in the aggregated structure [36] [37]. Thus, it is suggestion that the loading of the gold nanoparticles is Au@TiO$_2$/MCM-22 (PR) > Au/TiO$_2$/MCM-22 (DP) > Au/MCM-22, perfectly matching the ICP-AES result. An obvious absorption peak at 330 nm can be found in the spectrum of samples c, d and e, which is attributed to the extra-framework TiO$_2$ [38] and indicates that TiO$_2$ has doped on the support successfully.

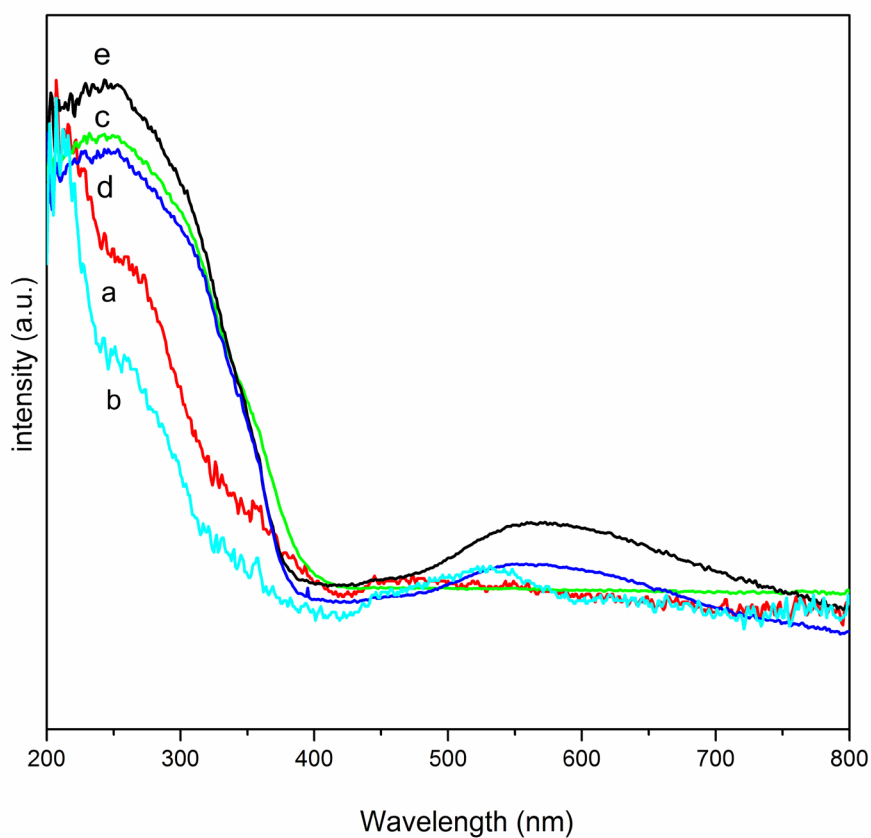### 3.2. Catalytic Oxidation of Cyclohexane

The catalytic performances of the above catalysts were investigated for cyclohexane oxidation. The blank experiment was carried out under the same reac-
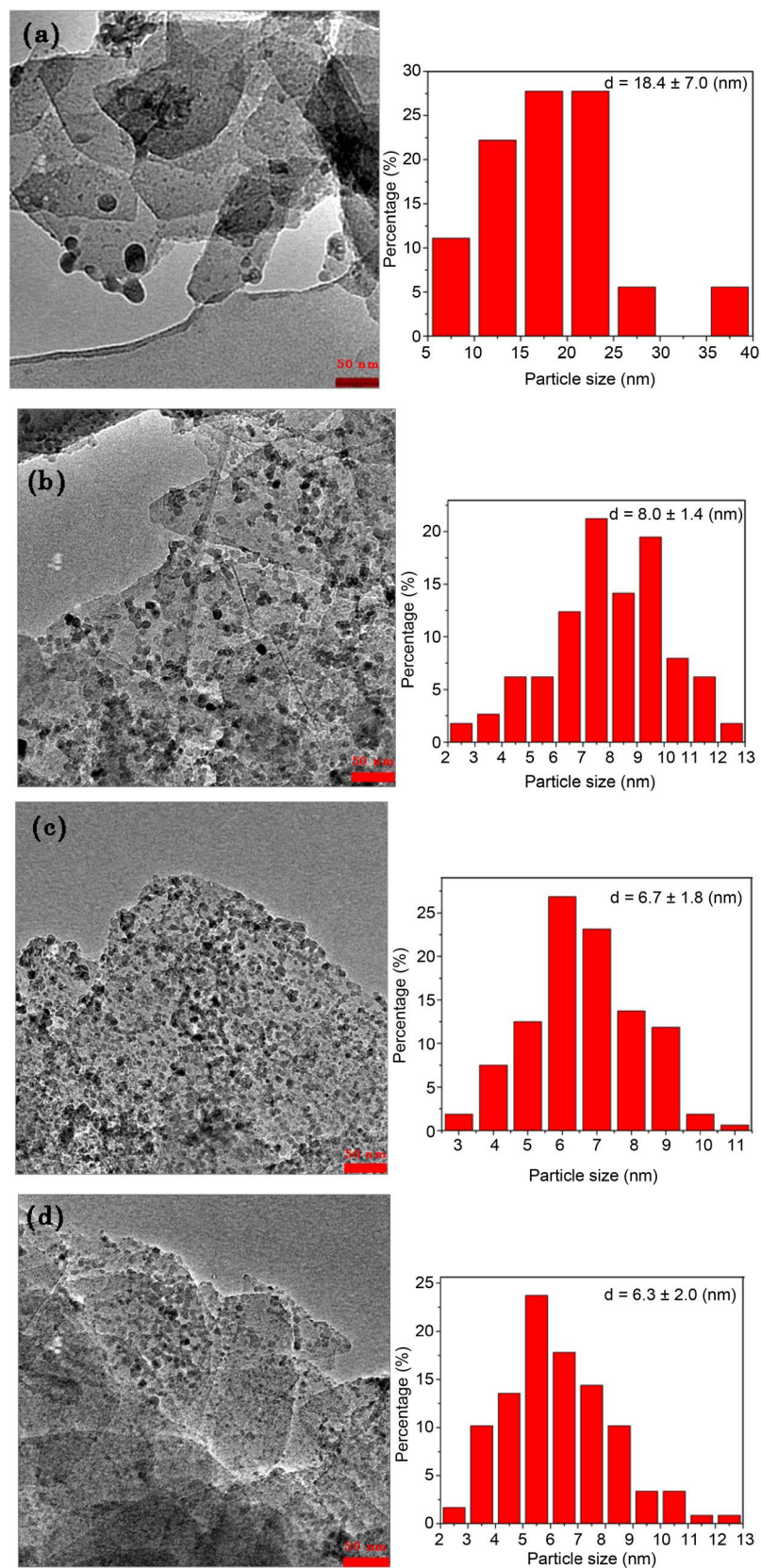
Figure 3. TEM images of catalysts. (a) Au/MCM-22 (DP); (b) Au@TiO$_2$/MCM-22 (DP); (c) Au@TiO$_2$/MCM-22 (PR); (d) Au@TiO$_2$/MCM-22 (PR) (repeated use four times). Au: 0.5 wt%.

Figure 4. UV-visible spectra of samples. (a) MCM-22; (b) Au/MCM-22; (c) TiO_2/MCM-22; (d) Au@TiO_2/MCM-22 (DP); (e) Au@TiO_2/MCM-22 (PR). Au: 0.5 wt%.

Table 3. The results of cyclohexane oxidation over different catalysts[a].

Entry	Catalyst	Conversion (%)	Total selectivity (%)	Product selectivity (%)[b]			
				K	A	CHHP	Others
1	Blank	4.05	81.26	43.71	20.04	17.51	18.74
2	MCM-22	6.78	74.78	29.92	25.15	19.71	25.22
3	TiO_2/MCM-22	7.27	77.11	31.13	26.99	18.99	22.89
4	Au/MCM-22	9.38	86.50	35.61	34.64	16.25	13.50
5	Au@TiO_2/MCM-22 (DP)	10.74	86.22	35.24	33.90	17.08	13.78
6	Au@TiO_2/MCM-22 (PR)	11.45	90.72	38.40	38.22	14.10	9.28

[a]Reaction conditions: cyclohexane (100 mL), catalyst (0.08 g), TBHP (0.4 g), pressure of O_2 (1.0 MPa), temperature (423 K), reaction time (1.0 h). [b]K: cyclohexanone; A: cyclohexanol; CHHP: cyclohexyl hydroperoxide; Others: acid and ester. Au: 0.5 wt%.

tion conditions. All the results are listed in Table 3. It is obvious that the reaction proceeds spontaneously (Table 3, Entry 1) and MCM-22 increases the conversion slightly at the cost of selectivity (Table 3, Entry 2). After TiO_2 was deposited on MCM-22, the catalytic activity of TiO_2/MCM-22 was improved because of the subsidiarity of TiO_2 (Table 3, Entry 2 and 3). The prepared gold catalysts

remarkably promote conversion and selectivity of cyclohexane oxidation simultaneously (Table 3, Entry 4 to 6), which confirms that the Au nanoparticles play an essential role in cyclohexane oxidation. Among all the gold catalysts, the Au@TiO$_2$/MCM-22 (PR) exhibits the best catalytic performance for the oxidation of cyclohexane, in respect of conversion and selectivity (Table 3, Entry 6). Remarkable differences can be observed in TOF of cyclohexanol oxidation catalyzed by different gold catalysts (Table 4). The nano-structured Au@TiO$_2$/MCM-22 (PR) exhibits extremely higher TOF than the reported gold catalysts [21] [39] [40]. Experiment results also show that the TOF become higher with a decrease in the amount of Au (Table 4). There are three main factors which can explain the excellent catalytic performance. Firstly, the synergistic effect between nano Au and nano TiO$_2$ plays a vital role. The interaction between the gold and the TiO$_2$ leads to the gold becoming electron-rich [41]. With the help of TiO$_2$, gold could activate oxygen more effectively. The outstanding oxygen storage capacity of TiO$_2$ will be beneficial to the catalytic performance of nano-Au@TiO$_2$ catalyst for cyclohexane oxidation. Secondly, the small particle size and even size distribution is another major reason for the prominent catalytic results. Thirdly, molecular sieve provides nano-Au@TiO$_2$ with high specific surface area place. Additionally, TiO$_2$ is a kind of reducible metal oxide that is able to store and release oxygen under oxygen rich and lean conditions, respectively [42]. It is indicated that the complex nano-structured catalyst Au@TiO$_2$/MCM-22 exhibits extremely higher TOF than the reported gold catalysts, although the catalytic performance of Au@TiO$_2$/MCM-22 prepared by photocatalytic reduction method is slightly superior to that of prepared by deposition precipitation method.

Table 4. TOF of different gold catalysts.

Catalyst	Au content (wt%)	TOF[k]	Reference
Au@TiO$_2$/MCM-22 (DP)[a]	0.5	48,889	This work
Au@TiO$_2$/MCM-22 (PR)[b]	0.5	52,121	This work
Au@TiO$_2$/MCM-41[c]	0.5	4503	[29]
Au/ZSM-5[d]	0.51	3096	[39]
Au/Al$_2$O$_3$[e]	0.6	4508	[21]
Au/MCM-41[f]	0.4	4550	[40]
Au@TiO$_2$/MCM-22 (PR)[g]	0.1	271,529	This work
Au@TiO$_2$/MCM-41 (PR)[h]	0.1	28,854	[29]
Au/Al$_2$O$_3$[i]	0.2	16,136	[21]
Au/TiO$_2$/SiO$_2$[j]	0.1	9723	[22]

[a]reaction conditions: cyclohexane 100 mL, catalyst 0.08 g, 423 K, 1.0 Mpa O$_2$, 1 h. [b]reaction conditions: cyclohexane 100 mL, catalyst 0.08 g, 423 K, 1.0 MPa O$_2$, 1 h. [c]reaction conditions: cyclohexane 100 mL, catalyst 0.02 g, 423 K, 1.0 Mpa O$_2$, 2.5 h. [d]reaction conditions: cyclohexane 2 mL, catalyst 0.005 g, 423 K, 1.0 MPa O$_2$, 3 h. [e]reaction conditions: cyclohexane 20 mL, catalyst 0.005 g, 423 K, 1.5 MPa O$_2$, 3 h. [f]reaction conditions: cyclohexane 2 mL, catalyst 0.005 g, 423 K, 1.0 MPa O$_2$, 6 h. [g]reaction conditions: cyclohexane 100 mL, catalyst 0.08 g, 423 K, 1.0 Mpa O$_2$, 1 h. [h]reaction conditions: cyclohexane 100 mL, catalyst 0.08 g, 423 K, 1.0 MPa O$_2$, 1 h. [i]reaction conditions: cyclohexane 20 mL, catalyst 0.05 g, 423 K, 1.5 Mpa O$_2$, 3 h. [j]reaction conditions: cyclohexane 20 mL, catalyst 0.05 g, 423 K, 1.5 MPa O$_2$, 1 h. [k]calculated by moles of cyclohexane converted per mole of Au per hour.

3.3. Recyclability Tests of the Prepared Catalyst

The recyclability tests were performed to evaluate the reused ability and stability of Au@TiO$_2$/MCM-22 (PR) in cyclohexane oxidation. At completion of each stage, the products were analyzed and the catalyst was recovered by filtration, thoroughly washed in ethanol, dried at 255 K, and then reused for a new set of cyclohexane oxidation experiment. The results in **Figure 5** show that there is little fluctuation of conversion or selectivity, namely, Au@TiO$_2$/MCM-22 (PR) performs good recyclability. We believe that the SMSI between Au and TiO$_2$ largely prevented the agglomeration of active sites during the oxidation reaction [43].

4. Conclusion

In summary, a novel gold nano-catalyst with nano-structured Au@TiO$_2$ has been successfully prepared. Nano-gold is immobilized on the nano-TiO$_2$ layer which is spread on the microporous molecular sieve MCM-22. Characterized results show that gold nanoparticles are immobilized on the substrate with small size (5 - 9 nm) and uniform dispersion. The complex nano-structured Au@TiO$_2$/ MCM-22 exhibits enhanced catalytic activity for cyclohexane oxidation. The catalytic performance of Au@TiO$_2$/MCM-22 prepared by photocatalytic reduction method is slightly superior to that of prepared catalyst by deposition precipitation. The outstanding catalytic performance could attribute to the synergistic effects of Au and TiO$_2$ in the complex nano-structured Au@TiO$_2$/MCM-22. The as-synthesized catalyst is chemically and mechanically robust and can be easily separated and reused. Supported noble metal nanoparticles catalysts (Pd, Pt, Ru, etc.) with the complex nano-structured Me@TiO$_2$
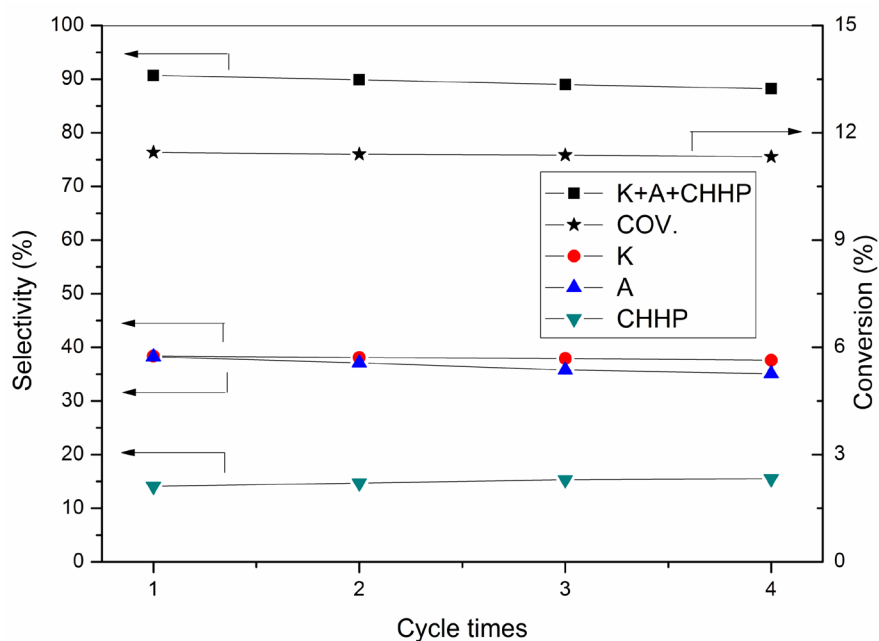
Figure 5. Effect of regeneration time on selective oxidation of cyclohexane.

could also be high efficient and be applied to different reaction systems. Recently, our group finds that nano-Pd@TiO$_2$ exhibits remarkably catalytic performance for hydrogenation of phenol under mild condition. We will also implement research on the nano-struc-ture Me@MO$_x$ (MO$_x$: metal oxides, such as CeO$_2$, ZnO, ZrO$_2$, etc.). The relative results will be revealed subsequently.

Acknowledgements

References

[1] Zhang, L., Blom, D.A. and Wang, H. (2011) Au-Cu$_2$O Core-Shell Nanoparticles: A Hybrid Metal-Semiconductor Heteronanostructure with Geometrically Tunable Optical Properties. *Chemistry of Materials*, **23**, 4587-4598.
https://doi.org/10.1021/cm202078t

[2] Goodman, D.W. (2005) "Catalytically Active Au on Titania:" Yet Another Example of a Strong Metal Support Interaction (SMSI)? *Catalysis Letters*, **99**, 1-4.
https://doi.org/10.1007/s10562-004-0768-2

[3] Costi, R., Saunders, A.E. and Banin, U. (2010) Colloidal Hybrid Nanostructures: A New Type of Functional Materials. *Angewandte Chemie International Edition*, **49**, 4878-4897. https://doi.org/10.1002/anie.200906010

[4] Cortie, M.B. and McDonagh, A.M. (2011) Synthesis and Optical Properties of Hybrid and Alloy Plasmonic Nanoparticles. *Chemical Reviews*, **111**, 3713-3735.
https://doi.org/10.1021/cr1002529

[5] Carbone, L. and Cozzoli, P.D. (2010) Colloidal Heterostructured Nanocrystals: Synthesis and Growth Mechanisms. *Nano Today*, **5**, 449-493.
https://doi.org/10.1016/j.nantod.2010.08.006

[6] Fu, Q. and Wagner, T. (2007) Interaction of Nanostructured Metal Overlayers with Oxide Surfaces. *Surface Science Reports*, **62**, 431-498.
https://doi.org/10.1016/j.surfrep.2007.07.001

[7] Maier, J. (2005) Nanoionics: Ion Transport and Electrochemical Storage in Confined Systems. *Nature Materials*, **4**, 805-815. https://doi.org/10.1038/nmat1513

[8] Diebold, U. (2003) The Surface Science of Titanium Dioxide. *Surface Science Reports*, **48**, 53-229. https://doi.org/10.1016/S0167-5729(02)00100-0

[9] Højrup-Hansen, K., Ferrero, S. and Henry, C.R. (2004) Nucleation and Growth Kinetics of Gold Nanoparticles on MgO (1 0 0) Studied by UHV-AFM. *Applied Surface Science*, **226**, 167-172. https://doi.org/10.1016/j.apsusc.2003.11.017

[10] Al-Abadleh, H.A. and Grassian, V.H. (2003) Oxide Surfaces as Environmental Interfaces. *Surface Science Reports*, **52**, 63-161.
https://doi.org/10.1016/j.surfrep.2003.09.001

[11] Chen, S. and Nickel, U. (1996) Synthesis of Hybrid Metal-Semiconductor Ultrafine Particles. Photochemical Deposition of Silver on a ZnO Colloid Surface. *Journal of the Chemical Society*, *Faraday Transactions*, **92**, 1555-1562.
https://doi.org/10.1039/FT9969201555

[12] Christy, A.J. and Umadevi, M. (2012) Synthesis and Characterization of Monodis-

persed Silver Nanoparticles. *Advances in Natural Sciences: Nanoscience and Nanotechnology*, **3**, Article ID: 035013.

[13] Tauster, S.J., Fung, S.C. and Garten, R.L. (1978) Strong Metal-Support Interactions. Group 8 Noble Metals Supported on Titanium Dioxide. *Journal of the American Chemical Society*, **100**, 170-175. https://doi.org/10.1021/ja00469a029

[14] Tauster, S.J., Fung, S.C., Baker, R.T.K. and Horsley, J.A. (1981) Strong Interactions in Supported-Metal Catalysts. *Science*, **211**, 1121-1125. https://doi.org/10.1126/science.211.4487.1121

[15] Li, Y.Z., Fan, Y.N., Yang, H.P., Xu, B.L., Feng, L.X., Yang, M.F. and Chen, Y. (2003) Strong Metal-Support Interaction and Catalytic Properties of Anatase and Rutile Supported Palladium Catalyst Pd/TiO$_2$. *Chemical Physics Letters*, **372**, 160-165. https://doi.org/10.1016/S0009-2614(03)00383-X

[16] Weerachawanasak, P., Praserthdam, P., Arai, M. and Panpranot, J. (2008) A Comparative Study of Strong Metal-Support Interaction and Catalytic Behavior of Pd Catalysts Supported on Micron- and Nano-Sized TiO$_2$ in Liquid-Phase Selective Hydrogenation of Phenylacetylene. *Journal of Molecular Catalysis A: Chemical*, **279**, 133-139. https://doi.org/10.1016/j.molcata.2007.10.006

[17] Vayenas, C.G., Brosda, S. and Pliangos, C. (2003) The Double-Layer Approach to Promotion, Electrocatalysis, Electrochemical Promotion, and Metal-Support Interactions. *Journal of Catalysis*, **216**, 487-504. https://doi.org/10.1016/S0021-9517(02)00127-6

[18] Fu, Q., Wagner, T., Olliges, S. and Carstanjen, H.-D. (2005) Metal-Oxide Interfacial Reactions: Encapsulation of Pd on TiO$_2$ (110). *The Journal of Physical Chemistry B*, **109**, 944-951. https://doi.org/10.1021/jp046091u

[19] Schuchardt, U., Cardoso, D., Sercheli, R., Pereira, R., de Cruz, R.S., Guerreiro, M.C., Mandelli, D., Spinace, E.V. and Fires, E.L. (2001) Cyclohexane Oxidation Continues to Be a Challenge. *Applied Catalysis A: General*, **211**, 1-17. https://doi.org/10.1016/S0926-860X(01)00472-0

[20] Weissermel, K. and Arpe, H.-J. (2003) Industrial Organic Chemistry. 4th Edition, Wiley-VCH, Weinheim. https://doi.org/10.1002/9783527619191

[21] Xu, L.X., He, C.H., Zhu, M.Q. and Fang, S. (2007) A Highly Active Au/Al$_2$O$_3$ Catalyst for Cyclohexane Oxidation Using Molecular Oxygen. *Catalysis Letters*, **114**, 202-205. https://doi.org/10.1007/s10562-007-9058-0

[22] Xu, L.X., He, C.H., Zhu, M.Q., Wu, K.J. and Lai, Y.L. (2007) Silica-Supported Gold Catalyst Modified by Doping with Titania for Cyclohexane Oxidation. *Catalysis Letters*, **118**, 248-253. https://doi.org/10.1007/s10562-007-9178-6

[23] Xu, L.X., He, C.H., Zhu, M.Q., Wu, K.J. and Lai, Y.L. (2008) Surface Stabilization of Gold by Sol-Gel Post-Modification of Alumina Support with Silica for Cyclohexane Oxidation. *Catalysis Communications*, **9**, 816-820. https://doi.org/10.1016/j.catcom.2007.09.005

[24] Wu, Y.J., Ren, X.Q., Lu, Y.D. and Wang, J. (2008) Rapid Synthesis of Zeolite MCM-22 by Acid-Catalyzed Hydrolysis of Tetraethylorthosilicate. *Materials Letters*, **62**, 317-319. https://doi.org/10.1016/j.matlet.2007.05.026

[25] Pan, X.Y. and Xu, Y.-J. (2013) Fast and Spontaneous Reduction of Gold Ions over Oxygen-Vacancy-Rich TiO$_2$: A Novel Strategy to Design Defect-Based Composite Photocatalyst. *Applied Catalysis A: General*, **459**, 34-40. https://doi.org/10.1016/j.apcata.2013.04.007

[26] Li, L., Jin, C., Wang, X.C., Ji, W.J., Pan, Y., van der Knaap, T., van der Stoel, R. and Au, C.T. (2009) Cyclohexane Oxidation over Size-Uniform Au Nanoparticles (SBA-15 Hosted) in a Continuously Stirred Tank Reactor Under Mild Conditions. *Cataly-*

sis Letters, **129**, 303-311. https://doi.org/10.1007/s10562-009-9853-x

[27] Yan, W.F., Chen, B., Mahurin, S.M., Schwartz, V., Mullins, D.R., Lupini, A.R., Pennycook, S.J., Dai, S. and Overbury, S.H. (2005) Preparation and Comparison of Supported Gold Nanocatalysts on Anatase, Brookite, Rutile, and P25 Polymorphs of TiO_2 for Catalytic Oxidation of CO. *The Journal of Physical Chemistry B*, **109**, 10676-10685. https://doi.org/10.1021/jp044091o

[28] Ismail, A.A., Hakki, A. and Bahnemann, D.W. (2012) Mesostructure Au/TiO_2 Nanocomposites for Highly Efficient Catalytic Reduction of p-Nitrophenol. *Journal of Molecular Catalysis A*: *Chemical*, **358**, 145-151. https://doi.org/10.1016/j.molcata.2012.03.009

[29] Zhou, J.C., Yang, X.F., Wang, Y.Q. and Chen, W.J. (2014) An Efficient Oxidation of Cyclohexane over Au TiO_2/MCM-41 Catalyst Prepared by Photocatalytic Reduction Method Using Molecular Oxygen as Oxidant. *Catalysis Communications*, **46**, 228-233. https://doi.org/10.1016/j.catcom.2013.12.026

[30] Izutsu, H., Nair, P.K., Maeda, K., Kiyozumi, Y. and Mizukami, F. (1997) Structure and Properties of TiO_2-SiO_2 Prepared by Sol-Gel Method in the Presence of Tartaric Acid. *Materials Research Bulletin*, **32**, 1303-1311. https://doi.org/10.1016/S0025-5408(97)00106-2

[31] Thangaraj, A., Kumar, R., Mirajkar, S.P. and Ratnasamy, P. (1991) Catalytic Properties of Crystalline Titanium Silicalites I. Synthesis and Characterization of Titanium-Rich Zeolites with MFI Structure. *Journal of Catalysis*, **130**, 1-8. https://doi.org/10.1016/0021-9517(91)90086-J

[32] Tuel, A. (1996) Crystallization of Titanium Silicalite-1 (TS-1) from Gels Containing Hexanediamine and Tetrapropylammonium Bromide. *Zeolites*, **16**, 108-117. https://doi.org/10.1016/0144-2449(95)00109-3

[33] Daniel, M.-C. and Astruc, D. (2004) Gold Nanoparticles: Assembly, Supramolecular Chemistry, Quantum-Size-Related Properties, and Applications toward Biology, Catalysis, and Nanotechnology. *Chemical Reviews*, **104**, 293-346. https://doi.org/10.1021/cr030698+

[34] Wu, P.P., Bai, P., Lei, Z.B., Loh, K.P. and Zhao, X.S. (2011) Gold Nanoparticles Supported on Functionalized Mesoporous Silica for Selective Oxidation of Cyclohexane. *Microporous and Mesoporous Materials*, **141**, 222-230. https://doi.org/10.1016/j.micromeso.2010.11.011

[35] Wu, P.P., Bai, P., Loh, K.P. and Zhao, X.S. (2010) Au Nanoparticles Dispersed on Functionalized Mesoporous Silica for Selective Oxidation of Cyclohexane. *Catalysis Today*, **158**, 220-227. https://doi.org/10.1016/j.cattod.2010.03.027

[36] Fang, J., Cao, S.-W., Wang, Z., Mehdi Shahjamali, M., Loo, S.C.J., Barber, J. and Xue, C. (2012) Mesoporous Plasmonic Au-TiO_2 Nanocomposites for Efficient Visible-Light-Driven Photocatalytic Water Reduction. *International Journal of Hydrogen Energy*, **37**, 17853-17861. https://doi.org/10.1016/j.ijhydene.2012.09.023

[37] Zhong, Z.Y., Patskovskyy, S., Bouvrette, P., Luong, J.H.T. and Gedanken, A. (2004) The Surface Chemistry of Au Colloids and Their Interactions with Functional Amino Acids. *The Journal of Physical Chemistry B*, **108**, 4046-4052. https://doi.org/10.1021/jp037056a

[38] Wang, M., Zhou, J.C., Mao, G.Y. and Zheng, X.L. (2012) Synthesis of TS-1 from an Inorganic Reactant System and Its Catalytic Properties for Allyl Chloride Epoxidation. *Industrial & Engineering Chemistry Research*, **51**, 12730-12738. https://doi.org/10.1021/ie202524t

[39] Zhao, R., Ji, D., Lv, G.M., Qian, G., Yan, L., Wang, X.L. and Suo, J.S. (2004) A Highly Efficient Oxidation of Cyclohexane over Au/ZSM-5 Molecular Sieve Catalyst

with Oxygen as Oxidant. *Chemical Communications*, **10**, 904-905.
https://doi.org/10.1039/b315098d

[40] Lü, G.M., Zhao, R., Qian, G., Qi, Y.X., Wang, X.L. and Suo, J.S. (2004) A Highly Efficient Catalyst Au/MCM-41 for Selective Oxidation Cyclohexane Using Oxygen. *Catalysis Letters*, **97**, 115-118.
https://doi.org/10.1023/B:CATL.0000038571.97121.b7

[41] Laursen, S. and Linic, S. (2009) Strong Chemical Interactions between Au and Off-Stoichiometric Defects on TiO_2 as a Possible Source of Chemical Activity of Nanosized Au Supported on the Oxide. *The Journal of Physical Chemistry C*, **113**, 6689-6693. https://doi.org/10.1021/jp810603u

[42] Widmann, D., Liu, Y., Schüth, F. and Behm, R.J. (2010) Support Effects in the Au-Catalyzed CO Oxidation—Correlation between Activity, Oxygen Storage Capacity, and Support Reducibility. *Journal of Catalysis*, **276**, 292-305.
https://doi.org/10.1016/j.jcat.2010.09.023

[43] Tan, H.T., Chen, Y.T., Zhou, C.M., Jia, X.L., Chen, J., Rui, X.H., Yan, Q.Y. and Yang, Y.H. (2012) Palladium Nanoparticles Supported on Manganese Oxide-CNT Composites for Solvent-Free Aerobic Oxidation of Alcohols: Tuning the Properties of Pd Active Sites Using MnOx. *Applied Catalysis B: Environmental*, **119-120**, 166-174. https://doi.org/10.1016/j.apcatb.2012.02.024

Scientific Research Publishing

Submit or recommend next manuscript to SCIRP and we will provide best service for you:

Accepting pre-submission inquiries through Email, Facebook, LinkedIn, Twitter, etc.
A wide selection of journals (inclusive of 9 subjects, more than 200 journals)
Providing 24-hour high-quality service
User-friendly online submission system
Fair and swift peer-review system
Efficient typesetting and proofreading procedure
Display of the result of downloads and visits, as well as the number of cited articles
Maximum dissemination of your research work

Submit your manuscript at: http://papersubmission.scirp.org/
Or contact mrc@scirp.org